

Applications of the Finite Element Method to Designing Composite Metamaterials

G. Mumcu[†] M. Valerio[†] K. Sertel[†] J.L. Volakis[†]

Abstract – We outline a fabrication and characterization process for composite materials exhibiting uniaxial anisotropy. Our proof-of-concept sample consists of alternating layers of high-contrast homogeneous dielectrics. We describe a finite element-based cavity measurement method to accurately characterize effects of adhesive loss in these assembled samples. In the latter half of the paper, we introduce a genetic optimization algorithm to design fairly complex composite material textures exhibiting unique field characteristics and dispersion. We conclude by proposing a methodology to design and fabricate metamaterial textures made of commercially available homogeneous ingredients. The automated design process is conjugated by automated fabrication of these designs using advanced material processing techniques such as low temperature co-fired ceramic processing, inkjet material printing, and robo-casting.

1 INTRODUCTION

Engineered metamaterial media have drawn considerable interest over the past 5 years by introducing uncommon possibilities to realize compact, low cost, high efficiency microwave components, antennas and arrays. Metamaterials typically consist of periodic textures formed by two or more isotropic materials. But, the use of anisotropic layers to form metamaterial volumes promises much greater design flexibility, including the molding of new k - ω diagrams. However, a challenge is the difficulty and expense to realize low loss anisotropic dielectric and ferromagnetic layers. To alleviate this, the first part of this paper will focus on the design of layered media that emulate anisotropic media. We will demonstrate a FEM design methodology with a cavity measurement setup to extract equivalent homogeneous material properties (tensor permittivity and accurate loss tangent) made up of thin isotropic layers of highly pure, low loss Alumina (Al_2O_3) and Barium Titanate (BaTiO_3) materials. The FEM is particularly important to accurately extract the material permittivity tensor using an iterative method. Loss tangents can be also determined from a return loss measurement once the cavity design is realized via the FEM.

An alternative approach to realize simple anisotropic materials is fabricating a “unit cell” texture of an engineered medium. Realization of such textured composites is within the reach of low-loss material manufacturing techniques, such as low temperature co-fired ceramics (LTCC), inkjet-like

material printers, and robo-casting of ceramic mixtures. In Section 4, we present an optimization approach using a genetic algorithm with a 3-dimensional FE-BI core solver (with periodic boundary conditions) to design a pre-defined transmission and reflection behavior. Such an approach should pave the way for realizing general metamaterial media with exotic properties including negative refraction index and frozen propagation modes [1].

2 REALIZATION AND CHARACTERIZATION OF LOW-LOSS ANISOTROPIC MATERIALS USING THIN CERAMIC LAMINATES

A simple artificial medium that emulates anisotropy can be created by constructing a periodic structure with different dielectric material layers [2]. At low frequencies where the periodicity is much smaller than the wavelength, the electrical behavior of such a structure can be characterized by using an effective permittivity tensor. As an example, here we consider the stack of alumina (Al_2O_3) – barium titanate (BaTiO_3) platelets as shown in Fig. 1. Due to different alternating layers, the stack in Fig. 1 has an effective uniaxial dielectric tensor of the form [2]

$$\bar{\epsilon}_r = \epsilon_{\perp} \bar{I} + (\epsilon_{//} - \epsilon_{\perp}) \hat{c}\hat{c}, \quad (1)$$

where $\epsilon_{//}$ is the dielectric constant along the distinguished axis (c- or // -axis), and ϵ_{\perp} is along the other two orthogonal directions (a- or \perp -axes). Before we proceed to use this engineered anisotropic

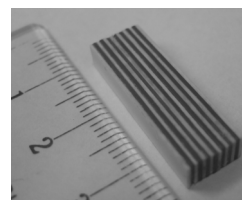


Figure 1: A 15-layer barium titanate (dark) – alumina (white) stack sample

material to build a more complex assembly, validation of well-known mixing rules (for calculating $\epsilon_{//}$ and ϵ_{\perp}) is in order. More importantly, the overall loss behavior of the layered material

[†] ElectroScience Lab., Dept. of Electrical and Computer Engineering, The Ohio State University, 1320 Kinnear Rd., Columbus, OH 43212.

including the effects of several bonding agents (adhesives) must be accurately characterized.

These characterization tasks can be carried out using a highly resonant cavity based measurement system [3]. Here, we use the FEM to compute the required properties of the resonant modes, such as resonant frequency, electric field filling ratio (stored energy within the sample as compared to the energy inside the overall sample loaded cavity system), and amount of cavity wall dissipation as compared to the overall stored energy (the G factor).

2.1 FEM based cavity measurement process

This simple and effective measurement setup consists of an enclosing cavity with the sample under test (SUT) placed in the middle. Resonant modes are excited through the cavity wall via an open ended coaxial probe whose location is determined to excite specific resonant modes (obtained from FEM simulations).

To compute the resonant field distributions and corresponding frequencies, the eigenvalues and eigenvectors of the Helmholtz equation for sample loaded cavity system

$$\nabla \times \nabla \times \mathbf{E}(\mathbf{r}) - k_0^2 \bar{\bar{\epsilon}}(\mathbf{r}) \cdot \mathbf{E}(\mathbf{r}) = 0 \quad (2)$$

must be solved. The choice of FEM to solve (2) is well justified when the flexibility of FEM in modeling arbitrary textures forming composite materials is considered. For this case, we discretize the cavity via a connected volumetric mesh of hexahedral elements (see [4] for details of FEM implementation using curvilinear hexahedral finite elements). Equation (2) is cast into a generalized eigenvalue system

$$\bar{\mathbf{A}}\mathbf{x} - \lambda\bar{\mathbf{B}}\mathbf{x} = 0 \quad (3)$$

using the discrete expansion of $\mathbf{E}(\mathbf{r})$ and applying Galerkin's testing. Principle permittivity values, $\epsilon_{//}$ and ϵ_{\perp} , are determined by matching the resonant frequencies calculated from FEM to those obtained from the nulls of measured return loss S_{11} . To do so, an iterative search is performed for the permittivity values used in FEM simulations. Once the permittivities are found, the loss factor is using the loaded quality factor of the cavity (see [3] for further details on the design of the resonant cavity and sensitivity of the setup).

Ignoring the cavity wall losses, the sensitivity of our setup for material loss tangent was 1×10^{-4} .

To validate the equivalent model of the layered stacks in 6 – 10 GHz range, we performed two FEM simulations when the layered stack shown in Fig. 1 is

placed in the middle of a copper cavity with dimensions 24, 12.8, and 80mm. The stack size was 7.6, 4, and 25mm, each layer being 0.508mm thick. In the first FEM simulation, individual layers of the stack were modeled by using manufacturer supplied dielectric constants of 82 for barium titanate and 9.6 for alumina. The second FEM simulation treated the overall stack as an equivalent uniaxial crystal with

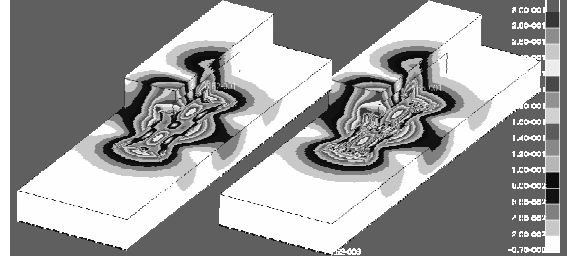


Figure 2: A resonant mode field distribution.

Left: Full wave model at 7.68 GHz; Right: Equivalent model at 7.53 GHz; The SUT shown in Fig. 1 is placed in the middle of the cavity.

effective permittivities of $\epsilon_{\perp} = 45.8$ and $\epsilon_{//} = 17.2$ obtained from [2] by using the manufacturer supplied dielectric constants. We indeed found a very good agreement within the resonant frequencies (2 – 3%) and field distributions. Fig. 2 depicts the similarity of a resonant field distribution within the sample loaded cavity for the full and equivalent models. Thus, the equivalent homogenous model for this medium can be used to characterize the loss. This provides a great ease in FEM simulations (due to less detailed geometry and meshing) that are required to iteratively match the calculated resonant frequencies to those measured in order to determine the permittivity values.

We calculated that the sample has a loss tangent of $\tan \delta = 8 \times 10^{-4}$ at 7.57 GHz when the layers were held together by means of two very thin straps. In case M Bond 610 (a two component phenolepoxy) glue was used, at the same frequency the loss increased to $\tan \delta = 1.6 \times 10^{-3}$. This comparison clearly shows the significant effect of minimal amount of glue introduced in the assembly, which needs to be taken into consideration when building such structures, especially for antenna applications where very small amount of loss may significantly degrade radiation efficiency.

3 ADVANCED MANUFACTURING APPROACHES

Today, several rapid prototyping alternatives exist for directly fabricating such assemblies. Low temperature co-fired ceramic processing is one of the most widely used, especially for THz applications.

Other alternatives, such as inkjet-like material printers for fabricating full 3-dimensional prototypes in a layer-by-layer fashion and the lesser known robo-casting, where a computer controlled drill shapes the mold that is simultaneously cast by a computer controlled tip are increasingly being used in ceramic processing. None of the above technologies require an adhesive agent (which typically introduces unwanted loss) to manufacture multi-dielectric textures. On the other hand, the purity levels of the ingredient materials and the stability of manufacturing processes (such as high temperature firing that may introduce cracks and defects) still introduce loss into the engineered samples. We are currently experimenting with inkjet printing techniques and building a robocasting system to fabricate more sophisticated material textures. These automated systems will be used in conjunction with automated design tools outlined in the following section.

4 METAMATERIAL DESIGN USING GENETIC OPTIMIZATION

These advances in material prototyping equipment open new possibilities for fabricating complex metamaterial textures. In the past, designs of metamaterial-like frequency-selective composite volumes have based on simple geometries due to the complexity of evaluating the characteristics of such designs. Yet to be seen characteristics are possible through automated design of such structures (e.g. see [5]). One such optimization process is outlined below where we wish to optimize the conductor geometry to obtain a specific frequency-selective behavior from the geometry shown in Fig. 3.

4.1 Sample Optimization Problem

As an example to illustrate this power of automated design, a genetic algorithm was used to optimize the transmission response of the frequency selective surface (FSS) having a unit cell depicted in Fig. 3.

The design is based on a loaded-fan element [6], and essentially consists of an inductive ring with inter-element coupling through an interdigital capacitor. It is desired that the conducting FSS geometry be printed on a single dielectric substrate and have a pass band at a given frequency. To accomplish this, we utilize a genetic optimization loop around the electromagnetic simulation.

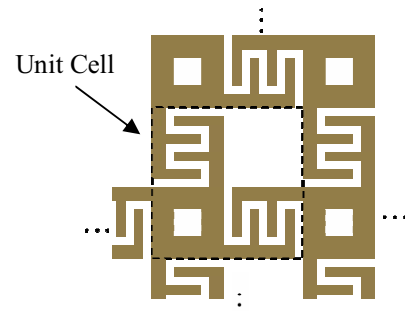


Figure 3: Geometry of the frequency selective surface based on a loaded fan element

4.2 Setup of the GA Optimizer

A genetic algorithm operates by keeping a list of chromosomes (essentially just binary strings) within a population. Each iteration in the genetic algorithm performs a number of operations on these chromosomes, such as selection, crossover, and mutation. Each chromosome in the population is assigned a fitness value to indicate how “good” it is. The genetic algorithm itself is quite general and problem-agnostic. Material designers can harness their creativity and provide problem-specific relationships between the chromosomes of the genetic algorithm and the input geometry of the simulation. Furthermore, a problem-specific calculation of the chromosome’s fitness value given the result of the simulation is also needed. By providing these two essential mappings (from chromosome to geometry and back from result to fitness), a wide variety of electromagnetic simulations can be optimized.

In this specific example, we map each chromosome with a variation of the loaded geometry fan shown in Fig. 3. The binary bits in the chromosome determine the width of the inductive ring, the length of each capacitive arm, and the spacing between each arm of the capacitor. Each chromosome’s string of 1’s and 0’s fully describes unique fan geometry as the input to the electromagnetic solver.

Once the geometry is evaluated via simulation, a fitness value is calculated from the transmission response. In this case, we perform a weighted average between an ideal frequency response (I), and the actual frequency response (a), with a set of weighting factors (w) to produce a measure of the curve “similarity”:

$$\sigma_c = \frac{\sum_{i=1}^N w_i (1 - |a_i - I_i|)}{\sum_{i=1}^N w_i} \quad (4)$$

A similar value can also be determined for the derivative of the actual frequency as compared to the derivative of the ideal response, so as not to equally reward those curves that cross at a specific point and those that run parallel. This value of curve similarity is stored in the fitness value of the chromosome whose mapped geometry produced the simulation result. In this way the genetic algorithm provides chromosomes with better fitness values (frequency response that is closer to the ideal response) with a higher probability of being selected to produce offspring in future generation.

It should be emphasized here that these particular choices of chromosome-to-geometry mappings and response-to-fitness mappings depend entirely on the optimization problem at hand. Other methods may prove more suitable for different problems, and some experimentation is necessary [7, 8].

4.3 Optimized Response

A genetic optimization was performed using the loaded fan geometry. The resulting transmission response for normal incidence is shown in Fig. 4. Both the ideal response and the best chromosome's response are shown to be in good agreement.

This optimization was completed in 11 hours with 24 computers using a distributed computing platform specifically designed for electromagnetic optimization [9].

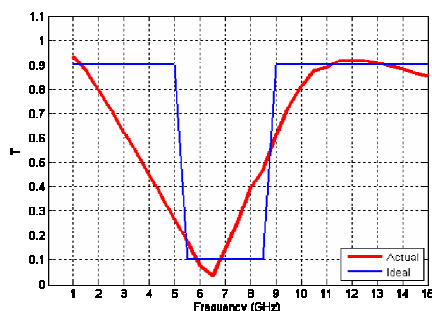


Figure 4: Ideal transmission response and optimized response of the loaded fan FSS

4 FUTURE WORK

We are currently improving our GA optimizer to design multi-dielectric material textures exhibiting

specific dispersion characteristics. This will be achieved via the design of the unit cell of the periodic structure made up of a specific arrangement of different material blocks. The FEM will be used to model the unit cell by imposing necessary periodic boundary conditions on the boundaries of the computational domain, resulting in a purely FEM approach (without the need to terminate the boundary via integral equations or absorbing boundary conditions). The resulting design will required to exhibit the desired dispersion diagram and the GA optimizer will be constrained to use only commercially available material blocks. With the help of advanced material processing techniques, such as inkjet material printing, we are aiming to manufacture and test these engineered material designs that are generated completely autonomously via the GA optimization process and computer controlled manufacturing.

References

- [1] G. Mumcu, K. Sertel, J. L. Volakis, I. Vitebskiy, and A. Figotin, "RF propagation in finite thickness unidirectional magnetic photonic crystals," *IEEE Transactions on Antennas and Propagation*, vol. 53, no. 12, pp. 4026–4034, Dec. 2005.
- [2] R. E. Collin, "A simple artificial anisotropic dielectric medium," *IRE Transactions on Microwave Theory and Techniques*, vol. 6, no. 2, pp. 206–209, 1958.
- [3] J. Krupka, K. Derzakowski, B. Riddle, and J. Baker-Jarvis, "A dielectric resonator for complex permittivity of low loss dielectric materials as a function of temperature," *Measurement Science and Technology*, vol. 9, no. 10, pp. 1751–1756, Oct. 1998.
- [4] G. E. Antilla and N. G. Alexopoulos, "Scattering from complex 3D geometries by a curvilinear hybrid finite element-integral equation approach," *J. Opt. Soc. Amer. A*, vol. 11, no. 4, pp. 1445–1457, 1994.
- [5] S. Koulouridis, D. Psychoudakis and J.L. Volakis, "Multi-Objective Optimal Antenna Design based on Volumetric Material Optimization," *IEEE Trans. Antennas Propagation*, Vol. 55, March 2007.
- [6] Y. E. Erdemli, K. Sertel, R. Gilbert, D. Wright, and J. L. Volakis, "Frequency Selective Surfaces to Enhance Performance of Broadband Reconfigurable Arrays," *IEEE Trans. Antenna Propagation*, vol. 50, No. 12, pp. 1716–1724, Dec. 2002.
- [7] J.L. Volakis, K. Sertel, and B.Usner, "Frequency Domain Hybrid Finite Element Methods in Electromagnetics" Morgan and Claypool, 2006, Chapter 5, pp. 109-131.
- [8] Y. Rahmat-Samii and E. Michielssen, *Electromagnetic Optimization by Genetic Algorithms*. New York: John Wiley, 1999.
- [9] M. D. Valerio and J. L. Volakis, "Design of Frequency Selective Surface as Antenna Ground Planes Using a Modular Distributed Optimization Framework," *IEEE Antennas and Propagation Society International Symposium, Honolulu, HI, June 2007*.